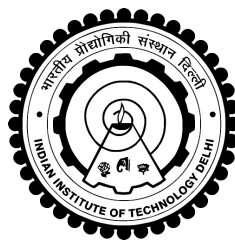


**STABILITY ANALYSIS OF AN ELECTROSPINNING JET
OF NEWTONIAN AND POLYMERIC FLUIDS**

DHARMANSH



**DEPARTMENT OF CHEMICAL ENGINEERING
INDIAN INSTITUTE OF TECHNOLOGY DELHI**

SEPTEMBER 2018

©Indian Institute of Technology Delhi (IITD), New Delhi, 2018

**STABILITY ANALYSIS OF AN ELECTROSPINNING JET
OF NEWTONIAN AND POLYMERIC FLUIDS**

by

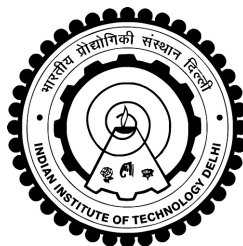
DHARMANSH

Department of Chemical Engineering

Submitted

in fulfillment of the requirements of the degree of Doctor of Philosophy

to the



INDIAN INSTITUTE OF TECHNOLOGY DELHI

September 2018

Dedicated to my family.....

Certificate

This is to certify that the thesis titled “**Stability Analysis of an Electrospinning Jet of Newtonian and Polymeric Fluids**” being submitted by **Mr. Dharmansh** in the Department of Chemical Engineering, Indian Institute of Technology Delhi for the award of the degree of **Doctor of Philosophy**, is a record of bona-fide research work carried out by him under my guidance and supervision. In my opinion, the thesis has reached the standards fulfilling the requirements of the regulations relating to the degree. The results contained in this thesis have not been submitted for the award of any other degree, associateship or similar title of any university or institution.

Dr. Paresh Chokshi

Associate Professor

Department of Chemical Engineering

Indian Institute of Technology Delhi

Acknowledgments

It is a pleasant task to express my thanks to all those who contributed in many ways to the successful completion of this thesis.

I would like to express my deep and sincere gratitude to my supervising guide Dr. Paresh Chokshi, for conceptualization of the subject and guidance, motivation and patience all the way through my doctoral research. I was extraordinarily fortunate in having the opportunity to work under him. He has supported me not only by providing research guidance over years, but also academically and emotionally through the rough road to finish this thesis. The joy and enthusiasm he has for research was contagious and motivational for me. Sir your valuable contributions will always be treasured.

I would like to thank the rest of my thesis committee: Prof. Rajesh Khanna, Prof. Anupam Shukla, and Dr. Bhanu Nandan, for their insightful comments and encouragement, but also for the hard question which helped me to widen my research from various perspectives.

My special regards to my teachers because of whose teaching at different stages of education has made it possible for me to see this day. Because of their kindness I feel, was able to reach a stage where I could write this thesis.

And most of all, I would like to share this moment of happiness with my loving, supportive, encouraging, family where the most basic source of my life energy resides. The support of my parents has been unconditional all these years and without their encouragement, prayers and understanding it would have been impossible for me to finish this work. I owe my deepest gratitude towards my better half for her eternal support and understanding of my goals and aspirations. Her patience and sacrifice will remain my inspiration throughout my life. It would be ungrateful on my part if I thank Preeti in these few words. I am thankful to my son Shivansh for giving me happiness during the last three years of my studies. I very fondly acknowledge my brother Vedansh, sister-in-law Sonia, sister Prachi and brother-in-law Saurabh for their love and support. I sincerely thank all my relatives who were with me for their love and encouragement.

Its my fortune to gratefully acknowledge the support of some special individuals. Words fail me to express my appreciation to my friend, Karan Gupta for technical and non technical discussions, understanding and valuable contributions in shaping the entire thesis. My most sincere gratitude to Chaitanya for helping me with important comments in thesis writing. I would like to thank Himanshu Gautam and Mohammad Wasil for their insightful inputs during the process modeling stage. My sincere and loving thanks to all my dear colleagues specially Ashutosh, Parvez, Richa, Rit Prateek, Supriya and Hari for being with me and their support.

I extend my thanks to all Chemical engineering staff, Krishnaji, Anita madam, Om Prakashji and Priyankaji for their support given during my research.

I gratefully acknowledge MHRD, Government of India for providing me financial support and IIT, Delhi to allow me to carryout my research in this esteemed institute.

This thesis has been kept on track and been seen through to completion with the support and encouragement of numerous people including my well wishers, friends and colleagues.

New Delhi

Dharmansh

Abstract

Electrospinning has emerged as a powerful and cost-effective technique to produce polymeric nanofibers for various technological applications. By subjecting the droplet of either polymer solution or molten polymer to an external electric field produces a strong tangential electric force which when exceeds the surface tension force creates a jet of polymeric fluid. The electric force generates a strong extensional flow field resulting in thinning of the jet. After traveling in a straight line path for a certain distance, the thinned jet undergoes whipping motion during which the solidification takes places leading to the collection of nanofibers at the bottom collector plate. Electrospinning often suffers from an axisymmetric instability which manifests in the form of thick-thin variations in fiber diameter along the fiber resulting in what is commonly referred to as the *beads-on-string* morphology. In the present study, the axisymmetric stability of an electrified jet is analyzed under electrospinning conditions using the linear stability theory. The unstable axisymmetric mode is believed to be responsible for the bead formation along the fibers, considered as a defect. This bead formation may be driven by two prevailing mechanisms, the classical capillary instability and the conducting instability. While the former is governed by the surface tension force, the latter is driven by the coupling of the electric field with the surface charges. Contrary to previous studies, which oversimplifies the electrified jet as a cylindrical jet with uniform radius, we analyze the stability of the realistic non-uniform thinning jet as observed in electrospinning experiments. The analysis examines both the Newtonian and the polymeric fluids with a finite electrical conductivity, modeled as a leaky dielectric medium. The stability of the thinning jet profile, obtained using the 1D slender body model, is analyzed by imposing non-periodic axisymmetric disturbances. The eigen-spectrum of the axisymmetric disturbance growth rate is constructed from the linearized disturbance equations discretized using the Chebyshev collocation technique.

For the Newtonian fluids, the thinning jet is found to be relatively less unstable than the uniform jet, which is attributed to the stabilizing role of extensional stress,

in addition to the axial variation in surface charge density and electric field, present in the non-uniform deforming jet, but ignored in the analysis of the uniform jet. The role of various process and material parameters, like electric field, electrical conductivity, surface tension, viscosity, is examined. The dominant mode for the thinning jet is an oscillatory conducting mode driven by the field-charge coupling. The disturbance energy balance finds the electric force to be the dominant force responsible for the disturbance growth potentially leading to bead formation along the fiber.

The stability analysis is further extended to incorporate the polymer rheology for two types of polymeric fluids, the low electrical conductivity PIB-based Boger fluid and the highly conductive PEO solution in ethanol/water. For the former fluid, the rheology is described using the Oldroyd-B model, suitable for unentangled polymers under weak elongational flow. On the other hand, the highly conductive polymer solution experiences a strong elongational flow due to very high axial electric force, for which case the viscoelasticity is appropriately described using the eXtended Pom-Pom (XPP) model, the nonlinear rheological model for entangled polymeric systems. For both the reference fluids considered, the analysis finds that polymer addition renders the jet stable and thus, suppresses bead formation during the straight jet path of electrospinning. Also, the enhancement in fluid elasticity, characterized by the flow Deborah number, plays a stabilizing role for the thinning jet of Oldroyd-B fluid. However, for the XPP fluid, the fluid elasticity shows a rich behavior with a stabilizing effect for moderate values of Deborah number, attributed to stretching of polymer chains between the branch points, and a destabilizing effect for highly elastic fluids, due to strain rate softening. Increasing the strain hardening effect in the polymer solution tends to stabilize the electrospinning jet, potentially producing smooth bead-less fibers. While the instability in low conductivity fluid is driven by capillary forces, the instability in the highly conductive fluid is an oscillatory conducting mode driven by the coupling of the surface charges and the axial electric field.

Further, the high temperature electrospinning process is studied by incorporation of the thermal effects. The heat transfer from the electrified jet to the surrounding is incorporated for both Newtonian and polymeric fluids. For Newtonian fluids, the cooling of the jet strongly enhances the viscosity of the fluid which tends to suppress the axisymmetric instability. Upon increasing the heat transfer coefficient, the leading growth rate of disturbances decreases and eventually changes its sign from positive to negative for both kinds of axisymmetric modes, the classical Rayleigh-Plateau mode and the conductivity mode. The stabilizing role of heat transfer is attributed to

the development of stabilizing viscous stresses in the jet. For polymeric fluids, the temperature dependence of both viscosity and relaxation time plays an important role in stability behavior of the jet in melt electrospinning. As the polymer melt analyzed, poly-lactic acid (PLA), is a low conductivity fluid with unentangled polymer molecules, the viscoelasticity is described using the non-linear rheological Giesekus constitutive model assuming very small axial conduction current. The growth rate corresponding to the leading mode in the eigenspectrum is found to increase with increasing surface tension forces and decrease with the enhanced external electric field. Thus, the leading growth rate behavior suggests that the classical Rayleigh-Plateau instability dominates over the conducting mode of instability for melt electrospinning. Further, the role of non-isothermal conditions in the stability behavior is examined. The convective heat transfer from electrified jet to the cooling ambiance leads to thicker fibers with greater stability to axisymmetric disturbances. The stabilizing effect of heat transfer is attributed mainly to the temperature sensitive fluid rheology. In particular, the enhancement in polymer viscosity in the jet propagation direction is responsible for the build up of stabilizing viscoelastic stress. The fluid elasticity, denoted by the flow Deborah number, also tends to stabilize the electrified jet as temperature drop along the flow increases the relaxation time of the polymer chains leading to high polymeric stress associated with the stretched chains.

The electrospinning of polymer solution is accompanied with the evaporation of solvent as the jet propagates towards the collector plate. As the jet thins due to electric force, the solvent evaporation becomes significant due to increased surface area of the jet. The modification in fluid rheology due to evaporation can play a significant role in controlling the axisymmetric instability of the jet. Hence, the solvent evaporation is incorporated in the stability analysis of the electrospinning jet of polymeric solution. While evaporation leads to thinner fiber due to loss of solvent, the increased polymer concentration builds up polymeric stresses leading to thicker fibers. The interplay of these two opposite effects of evaporation is also reflected in the stability behavior. The sensitivity of fluid rheology on its composition is found to play a dominant role in suppressing the growth rate of axisymmetric disturbances. Thus, the undesirable bead formation along the fiber can be eliminated by controlling the composition of the jet along its path achieved by controlling the rate of solvent evaporation.

Overall, we perform linear stability analysis of a non-cylindrical jet which undergoes thinning under electrospinning conditions to examine the axisymmetric instability potentially leading to either thick-thin variations in fiber diameter or beads-on-string morphology. The analysis is carried out for Newtonian fluids, polymer solution

and polymer melt subjected to realistic electrospinning conditions. Comprehensive knowledge of the stability behavior enables one to modify either the material properties or the processing conditions during electrospinning such that the axisymmetric instability is suppressed.

सारांश

इलेक्ट्रोस्पिनिंग विभिन्न तकनीकी अनुप्रयोगों के लिए बहुलक नैनोफाइबर का उत्पादन करने के लिए एक शक्तिशाली और लागत प्रभावी तकनीक के रूप में उभरा है। किसी भी बाहरी विद्युत क्षेत्र के प्रभाव में बहुलक की बूंद पर एक मजबूत स्पर्शिक विद्युत बल लगता है, जिसके पृष्ठ तनाव बल से अधिक होने पर बहुलक का एक जेट बनना आरम्भ होता है। विद्युत बल जेट की दिशा में मजबूत तनाव उत्पन्न करता है परिणामस्वरूप अंत में बहुत पतला जेट मिलता है। एक निश्चित दूरी के लिए एक सीधी रेखा पथ में यात्रा करने के बाद, पतला जेट घुमावदार गति से गुजरता है जिस दौरान ठोसकरण होता है और अंत में नीचे कलेक्टर प्लेट पर नैनोफाइबर मिलते हैं। इलेक्ट्रोस्पिनिंग में अक्सर धुरीसममित अस्थिरता जेट की दिशा के साथ फाइबर व्यास में मोटी-पतली विविधता के रूप में प्रकट होती है जिसे आमतौर पर बीड्स ऑन स्ट्रिंग के रूप में जाना जाता है। वर्तमान अध्ययन में, विद्युतीकृत जेट की धुरीसममित अस्थिरता का विश्लेषण रैखिक स्थिरता सिद्धांत का उपयोग करके इलेक्ट्रोस्पिनिंग स्थितियों के तहत किया गया है। धुरीसममित अस्थिरता को फाइबर के साथ बीड्स गठन के लिए ज़िम्मेदार माना जाता है। यह बीड्स गठन दो तरीके से घटित होता है, क्लासिक कॅपिलरी अस्थिरता और विद्युत चालकता अस्थिरता। प्रथम अस्थिरता का कारण पृष्ठ तनाव है, जबकि दूसरी अस्थिरता सतही विद्युत आवेश और विद्युत क्षेत्र के युग्मन से उत्पन्न होती है। पिछले अध्ययनों के विपरीत, जो विद्युतीकृत जेट को समान त्रिज्या वाले बेलनाकार जेट के रूप में मानते हैं, हम इलेक्ट्रोस्पिनिंग प्रयोगों में यथार्थवादी असमान पतले जेट की स्थिरता का विश्लेषण करते हैं। यह विश्लेषण न्यूटोनियन और बहुलक तरल पदार्थ दोनों को एक सीमित विद्युत चालकता के साथ जांचता है, जिसे लीकी डाइलेक्ट्रिक मॉडल का प्रयोग कर परिभाषित किया गया है असमान पतले जेट की स्थिर अवस्था, 1 डी मॉडल का उपयोग करके प्राप्त की जाती है, गैर-आवधिक धुरीसममित डिस्टर्बेन्स लगाकर इसका स्थिरता का विश्लेषण किया जाता है। डिस्टर्बेन्स वृद्धि दर का आइगन-स्पेक्ट्रम, चेबिस्हेव कोलाकेशन तकनीक का उपयोग करके विघटित रैखिक डिस्टर्बेन्स समीकरणों से बनाया गया है।

न्यूटोनियन तरल पदार्थ के लिए, पतला जेट एक समान त्रिज्या जेट से तुलनात्मक रूप से कम अस्थिर पाया जाता है, इसका मुख्य कारण एक्सटेंशनल तनाव का स्थिरता प्रभाव है। इसके अतिरिक्त सतह चार्ज घनत्व और विद्युत क्षेत्र में अक्षीय भिन्नता भी मुख्य कारण है जो कि समान जेट के विश्लेषण में अनदेखा किया गया है। विद्युत प्रक्रिया, विद्युत चालकता, पृष्ठ तनाव, श्यानता जैसी विभिन्न प्रक्रियाओं और भौतिक मानकों की भूमिका की जांच की जाती है। पतले जेट के लिए अस्थिरता का प्रमुख प्रकार फ़िल्ड-चार्ज युग्मन द्वारा संचालित एक ऑसीलेटरी अस्थिरता है। डिस्टर्बेन्स ऊर्जा संतुलन से विद्युत बल को प्रभावी बल के रूप में जिम्मेदार ठहराया जा सकता है जिससे संभावित रूप से फाइबर के साथ बीड्स गठन हो सकता है।

स्थिरता विश्लेषण को दो प्रकार के बहुलक तरल पदार्थ, कम विद्युत चालकता पीआईबी आधारित बोगर तरल पदार्थ और इथेनॉल / पानी में अत्यधिक प्रवाहकीय पीईओ के लिए आगे बढ़ाया जाता है। पूर्व तरल पदार्थ के लिए, रियोलाॅजी को ओल्ड्रॉइड-बी मॉडल का उपयोग करके वर्णित किया गया है, जो कमजोर

एक्सटेंडेड प्रवाह के तहत असंतुलित बहुलक के लिए उपयुक्त है। दूसरी तरफ, अत्यधिक प्रवाहकीय बहुलक बहुत उच्च अक्षीय विद्युत बल के कारण बहुत एक्सटेंडेड प्रवाह का अनुभव करता है, जिसके लिए श्यानता को एक्सटेंडेड पोम-पोम (XPP) मॉडल का उपयोग करके उचित रूप से वर्णित किया गया है, यह नॉनलिनेअर रियोलाॅजिकल मॉडल एनटॅगल्ड बहुलक के लिए उपयुक्त है। दोनों संदर्भ तरल पदार्थों के लिए, विश्लेषण में पाया गया है कि बहुलक मिलाना जेट को स्थिर करता है और इस प्रकार, इलेक्ट्रोस्पिनिंग के सीधे जेट पथ के दौरान बीड्स गठन को कम करता है। इसके अलावा, प्रवाह De द्वारा इलॅस्टिसिटी में वृद्धि, ओल्ड्रॉइड-बी तरल पदार्थ के पतले जेट के लिए एक स्थिर भूमिका निभाता है। हालांकि, XPP तरल पदार्थ के लिए, इलॅस्टिसिटी, De के मध्यम मूल्यों के लिए स्थिर प्रभाव के साथ एक समृद्ध व्यवहार दिखाती है, जो शाखा बिंदुओं के बीच बहुलक श्रृंखलाओं को खींचने के लिए जिम्मेदार ठहराती है, और अत्यधिक इलॅस्टिसिटी तरल पदार्थ के लिए तनाव दर नरम होने के कारण एक अस्थिर भूमिका निभाता है। बहुलक में स्ट्रेन हार्डनिंग प्रभाव में वृद्धि इलेक्ट्रोस्पिनिंग जेट को स्थिर करने के लिए होती है, संभावित रूप से इलॅस्टिसिटी कम बीड्स वाले फाइबर का उत्पादन करती है। जबकि कम चालकता तरल पदार्थ में अस्थिरता कॅपिलरी बलों द्वारा संचालित होती है, अत्यधिक प्रवाहकीय तरल पदार्थ में अस्थिरता सतह के चार्जस और अक्षीय विद्युत क्षेत्र के युग्मन द्वारा संचालित एक ऑसीलेटरी मोड है।

इसके अलावा, उच्च तापमान इलेक्ट्रोस्पिनिंग प्रक्रिया का अध्ययन थर्मल प्रभावों को शामिल करके किया जाता है। विद्युतीकृत जेट से आस-पास के गर्मी हस्तांतरण को न्यूटोनियन और बहुलक तरल पदार्थ दोनों के लिए शामिल किया गया है। न्यूटोनियन तरल पदार्थ के लिए, जेट की ठंडक तरल पदार्थ की श्यानता को दृढ़ता से बढ़ाती है जो धुरीमित अस्थिरता को दबाने के लिए प्रेरित होती है। गर्मी हस्तांतरण गुणांक को बढ़ाने पर, डिस्टर्बेन्स की अग्रणी वृद्धि दर कम हो जाती है और अंततः धुरीसममित अस्थिरता, क्लासिक कॅपिलरी अस्थिरता और विद्युत चालकता अस्थिरता दोनों प्रकार के लिए स्थिर से अस्थिर हो जाती है।

गर्मी हस्तांतरण की स्थाई भूमिका को जेट में श्यानता तनाव को जिम्मेदार ठहराया जाता है। बहुलक तरल पदार्थ के लिए, श्यानता और इलॉस्टिसिटी दोनों की तापमान निर्भरता मेल्ट इलेक्ट्रोस्पिनिंग में जेट के स्थिरता व्यवहार में एक महत्वपूर्ण भूमिका निभाता है। चूंकि मेल्ट पॉलिमर, पॉली-लैक्टिक एसिड (पीएलए), बिना किसी पृथक बहुलक अणुओं के साथ कम चालकता तरल पदार्थ होता है, विस्को-इलास्टिसिटी को गैर-रैखिक रियोलॉजिकल जेईसेकस मॉडल का उपयोग करके वर्णित किया आइगन –स्पेक्ट्रम में अग्रणी मोड से संबंधित विकास पृष्ठ तनाव के साथ बढ़ती है तथा विद्युत क्षेत्र के साथ घटती है। इस प्रकार, अग्रणी विकास दर व्यवहार से पता चलता है कि, क्लासिक कॅपिलरी अस्थिरता इलेक्ट्रोडोस्पिनिंग के लिए अस्थिरता का संचालन करती है। इसके अलावा, स्थिरता व्यवहार में असमान तापमान की स्थितियों की भूमिका की जांच की जाती है। तापमान संवेदनशील द्रव रियोलॉजी को मुख्य रूप से गर्मी हस्तांतरण के स्थिरीकरण प्रभाव के लिए जिम्मेदार ठहराया जाता है। विशेष रूप से, जेट प्रसार दिशा में बहुलक श्यामलता में वृद्धि विस्को-इलास्टिसिटी तनाव के स्थिर करने के निर्माण के लिए जिम्मेदार है। इलास्टिसिटी, जो De द्वारा दर्शाया गया है, भी विद्युतीकृत जेट को स्थिर करने के लिए जाना जाता है क्योंकि प्रवाह के साथ कम तापमान बहुलक श्रृंखलाओं के विश्राम समय को बढ़ाता है जिससे बड़ी हुई श्रृंखलाओं से जुड़े उच्च बहुलक तनाव में रहते हैं।

बहुलक विलयन की इलेक्ट्रोस्पिनिंग विलायक के वाष्पीकरण के साथ होती है जैसे जेट कलेक्टर प्लेट की तरफ बढ़ता है। विद्युत बल के प्रभाव में जेट के बढ़ते सतह क्षेत्र के कारण विलायक वाष्पीकरण महत्वपूर्ण हो जाता है। वाष्पीकरण के कारण द्रव रियोलॉजी में संशोधन जेट की धुरीमित अस्थिरता को नियंत्रित करने में महत्वपूर्ण भूमिका निभा सकता है। इसलिए, विलायक वाष्पीकरण बहुलक के इलेक्ट्रोस्पिनिंग जेट के स्थिरता विश्लेषण में शामिल किया गया है। वाष्पीकरण विलायक के नुकसान के कारण पतले फाइबर की ओर जाता है, जबकि बड़ी हुई बहुलक सांद्रता, बहुलक में तनाव पैदा करती है। वाष्पीकरण के इन दो विपरीत प्रभावों का अंतःक्रिया, स्थिरता व्यवहार में भी दिखाई देता है। जेट की संरचना पर द्रव रियोलॉजी की संवेदनशीलता, अक्षीय डिस्टर्बेन्सस की वृद्धि दर को दबाने में एक प्रमुख भूमिका निभाती है। इस प्रकार, फाइबर के साथ अवांछनीय बीड्स गठन को विलायक वाष्पीकरण की दर को नियंत्रित करके जेट की संरचना को नियंत्रित करके समाप्त किया जा सकता है।

कुल मिलाकर, हम एक गैर-बेलनाकार जेट के रैखिक स्थिरता विश्लेषण को निष्पादित करते हैं जो धुरीसम्ममित अस्थिरता की जांच करने के लिए इलेक्ट्रोस्पिनिंग स्थितियों के तहत पतला हो जाता है जिससे संभावित रूप से फाइबर व्यास या बीड्स-ऑन-स्ट्रिंग मॉर्फोलॉजी में मोटी-पतली भिन्नताएं होती हैं। न्यूटोनियन तरल पदार्थ, बहुलक विलयन और मेल्ट बहुलक के लिए यथार्थवादी इलेक्ट्रोस्पिनिंग स्थितियों के अधीन विश्लेषण किया जाता है। स्थिरता व्यवहार का व्यापक ज्ञान इलेक्ट्रोस्पिनिंग के दौरान भौतिक

गुणों या प्रसंस्करण स्थितियों को संशोधित करने में सक्षम बनाता है जिससे धुरीमेट्रिक अस्थिरता को दबा दिया जाता है।

Table of contents

Certificate	i
Acknowledgements	iii
Abstract	v
Table of contents	ix
List of figures	xiii
List of tables	xvii
List of symbols	xix
1 Introduction	1
1.1 Motivation	1
1.2 Electrospinning process	3
1.3 Electrospinning parameters	7
1.3.1 Material parameters	8
1.3.2 Process parameters	10
1.3.3 Ambient parameters	12
1.4 Modeling of electrospinning	13
1.5 Stability analysis of electrospinning	14
1.6 Knowledge gaps	17
1.7 Research objectives	20
1.8 Thesis organization	22
2 Stability analysis of an electrified jet of Newtonian fluid	25
2.1 Introduction	26
2.2 Problem formulation	28
2.2.1 Steady-state solution	30
2.3 Linear stability analysis	34
2.3.1 Stability analysis of a uniform jet	34
2.3.2 Stability analysis for a thinning jet	35
2.4 Energy analysis	46

2.5	Conclusion	49
3	Stability analysis of electrospinning of a polymeric fluid	51
3.1	Introduction	52
3.2	Problem formulation	56
3.2.1	Linear rheological model: Oldroyd-B model	58
3.2.2	Non-linear rheological model: XPP model	59
3.2.3	Boundary conditions	60
3.2.4	Linear stability analysis	61
3.3	Steady-state solution	65
3.3.1	Low conductivity fluid: Oldroyd-B model	66
3.3.2	High conductivity fluid: XPP model	68
3.4	Linear stability analysis	70
3.4.1	Low conductivity polymer solution: Linear rheological model	70
3.4.2	High conductivity polymer solution: Nonlinear rheological model	77
3.5	Disturbance energy analysis	85
3.6	Conclusion	86
4	Non-isothermal electrospinning of a Newtonian fluid	89
4.1	Introduction	90
4.2	Modeling of the electrified jet	92
4.2.1	Problem formulation	92
4.2.2	Linear stability theory for non-isothermal jet	97
4.3	Results and discussion	99
4.3.1	Steady-state solution	99
4.3.2	Stability analysis	102
4.4	Conclusion	111
5	Non-isothermal electrospinning of a polymer melt	113
5.1	Introduction	114
5.2	Modeling of melt electrospinning	118
5.2.1	Problem formulation	118
5.2.2	Linear stability theory for non-isothermal jet	124
5.3	Results and discussion	126
5.3.1	Steady-state solution	126
5.3.2	Stability analysis	128
5.4	Conclusion	138

6	Electrospinning of polymer solution with solvent evaporation	141
6.1	Introduction	142
6.2	Formulation of the electrified jet with evaporation	145
6.2.1	Linear rheological model: Oldroyd-B model	148
6.2.2	Non-linear rheological model: XPP model	149
6.2.3	Boundary conditions	152
6.2.4	Stability analysis	153
6.3	Results and discussion	156
6.3.1	Low conductivity solution	156
6.3.2	High conductivity solution	163
6.4	Conclusion	170
7	Stability analysis of bilayer skin-core electrospinning	173
7.1	Introduction	174
7.2	Formulation of the skin-core electrified jet	175
7.2.1	Modeling of the skin-core electrified jet	175
7.2.2	Stability analysis of an electrified skin-core cylindrical jet	182
7.3	Results and discussion	183
7.3.1	Validation	183
7.3.2	Effect of external electric field on the bilayer jet stability	185
7.3.3	Role of core fluid volume fraction in jet instability	186
7.3.4	Influence of ratio of material properties on distinct instability modes	188
7.4	Conclusion	191
8	Conclusion and future scope	195
	Appendix	201
	Bibliography	206
	Thesis based publications	223
	Author resume	225

List of figures

1.1	Schematic diagram of electrified jet in electrospinning set-up	4
1.2	Bead formation on electrospinning fibers	8
1.3	Idealized XPP molecule	19
2.1	Schematic diagram of electrified jet in electrospinning set-up for Newtonian fluid	29
2.2	Steady-state profiles of the thinning jet for low conductive Newtonian fluid	32
2.3	Variation of various forces along the jet direction for Newtonian fluid	33
2.4	Real part of the growth rate against the disturbance wavenumber for a uniform jet	35
2.5	Eigenspectrum of disturbance growth rate for low conductive uniform Newtonian jet	37
2.6	Eigenspectrum of disturbance growth rate for low conductive thinning Newtonian jet	38
2.7	Eigenfunction of radius disturbance for Newtonian jet	40
2.8	Eigenspectrum of disturbance growth rate for high conductive uniform Newtonian jet	41
2.9	Eigenspectrum of disturbance growth rate for high conductive thinning Newtonian jet	42
2.10	Effect of Weber number on real part of the leading growth rate	43
2.11	Effect of electric field on real part of the leading growth rate	43
2.12	Effect of electrical conductivity on real part of the leading growth rate	44
2.13	Effect of Reynolds number on real part of the leading growth rate	45
2.14	Variation of interfacial electric stress with E_∞ and Péclet number	46
2.15	Variation in rate of change in total kinetic energy and various contributions to disturbance energy with external field strength	47
2.16	Variation in rate of change in total kinetic energy and various contributions to disturbance energy with Reynolds number	48

3.1	Schematic diagram of electrified straight jet in electrospinning set-up for polymer solution	57
3.2	Steady-state profiles of the thinning jet of PIB-based Boger fluid . . .	67
3.3	Steady-state profiles of the thinning jet of highly conductive PEO solution	69
3.4	Real part of the growth rate against the disturbance wavenumber for a uniform jet for PIB Boger fluid	71
3.5	Eigenspectrum of disturbance growth rate for PIB boger fluid for a uniform jet	72
3.6	Eigenspectrum of disturbance growth rate for PIB boger fluid for a thinning jet	73
3.7	Effect of flow Deborah number on the leading growth rate for the Oldroyd-B model for PIB Boger fluid	74
3.8	Steady-state profile of axial polymeric stress, for PIB Boger fluid for different Deborah number	75
3.9	Effect of polymer concentration on the leading growth rate for the Oldroyd-B model	76
3.10	Eigenspectrum of disturbance growth rate for a thinning jet of PEO solution modeled as XPP fluid	78
3.11	Effect of polymer concentration parameter, r_η , on the real part of the leading growth rate, ω_r for both uniform as well as thinning jet of the XPP fluid. Parameter: Set-II	80
3.12	Effect of fluid elasticity on the leading growth rate, for PEO solution modeled as the XPP fluid	81
3.13	Extensional viscosity against extension rate for the XPP model for different values of strain hardening parameter q	82
3.14	Effect of strain hardening parameter q on the real part of the leading growth rate for the XPP model	83
4.1	Various forces along the jet-direction for non-isothermal Newtonian jet	99
4.2	Steady-state profile (radius) of the non-isothermal Newtonian jet . . .	100
4.3	Steady-state profile (surface charge density) of the non-isothermal Newtonian jet	101
4.4	Steady-state profile of thinning jet with variation in activation energy for high viscosity fluid	102
4.5	Steady-state profile of thinning jet with variation in Biot number for high viscosity fluid	103

4.6	Eigenspectrum for isothermal and non-isothermal cases for low viscosity Newtonian fluid	104
4.7	Eigenspectrum for isothermal and non-isothermal cases for high viscosity Newtonian fluid	105
4.8	Influence of Bi on real part of the leading growth rate for Newtonian jet	105
4.9	Influence of activation energy on real part of the leading growth rate for Newtonian jet	106
4.10	Influence of air velocity on real part of the leading growth rate for thinning jet	107
4.11	Influence of E_∞ on real part of the leading growth rate for thinning jet	108
4.12	Effect of conductivity on real part of the leading growth rate for Newtonian jet	108
4.13	Influence of surface tension on real part of the leading growth rate for Newtonian jet	109
4.14	Maximum growth rate of disturbance corresponding to thinning jet and uniform jet	110
5.1	Schematic of non-isothermal electrospinning process	118
5.2	Steady-state profiles comparison of electrified jet obtained in the present study with literature	127
5.3	Steady-state profiles of electrified jet for polymer melt	128
5.4	Eigen-spectrum of disturbance growth rate for the electrospinning condition of PLA melt	130
5.5	Effect of surface tension and external electric field on the leading growth rate for PLA melt	131
5.6	Eigen-spectrum of disturbance growth rate for the electrospinning condition listed as Set-II	132
5.7	Effect of dimensionless heat transfer coefficient on the leading growth rate for PLA melt	134
5.8	Effect of heat transfer, in terms of Biot number, on steady-state jet profiles	134
5.9	Variation in local Biot number, Bi_L along the jet axis for different values of air velocity for polymer melt	135
5.10	Effect of ambient temperature on the leading growth rate, ω_r for polymer melt	136
5.11	Effect of fluid elasticity, at the nozzle temperature and elongational elasticity	137

5.12	Effect of fluid elasticity, in terms of Deborah number, on steady-state jet profiles	138
6.1	Schematic diagram of electrospinning process with evaporation	146
6.2	Steady-state profiles of electrified jet with axial direction with evaporation for Oldroyd-B model	158
6.3	Influence of mass transfer on the steady-state profiles of electrified jet for Oldroyd-B model	159
6.4	Influence of evaporation on the eigen-spectrum of disturbance growth rate, for Set-I	160
6.5	Influence of the evaporation on the stability of the electrified jet for Set-I	162
6.6	Steady-state profiles of electrified jet with axial direction with evaporation for XPP model	164
6.7	Influence of mass transfer on the steady-state profiles of electrified jet for XPP model	166
6.8	Influence of evaporation on the eigen-spectrum of disturbance growth rate, for Set-II	167
6.9	Influence of the evaporation on the stability of the electrified jet for Set-II	169
6.10	Influence of solvent loss on Deborah number and Pécletnumber of the polymer solution	170
7.1	Schematic diagram of electrospinning process with two fluid.	175
7.2	Force balance for core and skin fluids	178
7.3	Comparison between dispersion curves (ω_r vs. k) of the single fluid and the skin-core system	184
7.4	Influence of the external electric field on the bilayer jet instability . .	185
7.5	Influence of the radius variation of core fluid on the bilayer jet instability for different surface tension ratios of two fluid	187
7.6	Influence of the radius variation of core fluid on the bilayer jet instability for different conductivity ratios of two fluid	188
7.7	Influence of the surface tension ratio of core-skin fluids on the stability of the bilayer jet	189
7.8	Influence of the conductivity ratio of the core-skin fluids on the stability of the bilayer jet	191
7.9	Influence of the viscosity ratio, η_r , of two fluids on the bilayer jet . . .	192
8.1	derivation	202

List of tables

1.1	Various polymeric systems used in electrospinning (any suitable rheological model can be employed based on their rheological characterization).	5
1.2	Polymer used in melt electrospinning (suitable model can be used based on their rheological properties)	7
2.1	List of dimensionless groups.	30
3.1	List of dimensionless groups for Set-I (PIB Boger fluid) and Set-II (2 wt. % PEO in ethanol/water)	66
3.2	Energy budget for 2% by wt. PEO solution in ethanol (Set-II)	85
4.1	List of dimensionless groups for non-isothermal Newtonian jet.	96
5.1	List of dimensionless groups	123
6.1	List of dimensionless groups for Set-I (PIB Boger fluid) and Set-II (2 wt. % PEO in ethanol/water)	151
7.1	Dimensionless groups for the skin core Newtonian fluid jet with the values used in the current analysis	183

List of symbols

Symbol	Definition
g	Gravity constant
h_0	Heat transfer coefficient of jet material
k	Axial wave number of the disturbances
k_T	Thermal conductivity of jet materials
ka	conductivity constant
m	Mass transfer coefficient
q	Number of branches at backbone ends (XPP parameter)
r	XPP molecule relaxation time ratio (backbone orientation/stretch)
r_η	Polymer viscosity ratio
t	Time co-ordinate (fast time scale)
v	Dimensionless velocity of the jet
v_0	Dimensional jet velocity at nozzle-exit
\bar{v}	Steady-state profile of fluid velocity through the jet
\tilde{v}	Disturbance profile of fluid velocity through the jet
z	Dimensionless axial co-ordinate
B_0	Bond number
Bi	Biot number
C_p	Heat capacity of the jet material
Ca	Capillary number
De	Deborah number
E	Dimensionless electric field along the jet
E_0	Dimensional jet electric field at nozzle-exit
E_n	Normal electric field through jet
E_t	Tangential electric field through jet
\bar{E}	Steady-state profile of electric field through jet
\tilde{E}	Disturbance profile of electric field through jet
\bar{E}_n	Normal electric field through air

\bar{E}_t	Tangential electric field through air
E_a	Dimensionless activation energy
E_{a^*}	Dimensional activation energy
E_∞	Imposed potential difference
F	Viscoelastic function in XPP model
Fr	Froude number
G	Elastic moduli of polymer
I	Current passing through the jet
K	Electrical conductivity of the jet solution
K_r	Conductivity ratio of two fluids
KE	Total kinetic energy
L	Length of the straight jet
M	Mass Stanton No.
N	Number of collocation points
Na	Nahme-Griffith number
Pe	Electric Pécletnumber
Pe^T	Thermal Pécletnumber
Q	Volumetric flow rates at nozzle-exit
R	Dimensionless radius of the jet
R_0	Dimensional jet radius at nozzle-exit
\bar{R}	Steady-state profile of jet radius
\tilde{R}	Disturbance profile of jet radius
R_{ig}	Ideal gas constant
Re	Reynolds number
T	Dimensionless straight jet temperature
T_0	Material temperature at nozzle-exit (reference)
T_a	Dimensionless temperature of cooling air
T_g	Glass transition temperature
χ	Jet aspect ratio
V_{air}	Air velocity
We	Weber number
\mathcal{C}	Energy from convection forces
\mathcal{E}	Energy from electric forces
\mathcal{P}	Energy from polymeric forces
\mathcal{S}	Energy from surface-tension forces

Greek symbols

α	Field strength
α_m	Mobility factor (Giesekus model)
β	Relative Permittivity of the jet solution with air
γ	Surface-tension of the fluid
γ_r	Surface-tension ratio of two fluids
ϵ	Permittivity of the jet solution
$\bar{\epsilon}$	Permittivity of the air
η	Viscosity of the fluid
η_p	Viscosity of the polymer component
η_s	Viscosity of the solvent component
η_a	Viscosity constant
η_b	Viscosity constant
η_c	Viscosity constant
η_d	Viscosity constant
η_r	Viscosity ratio of two fluids
λ	Relaxation time of polymer system
λ_a	Relaxation time constant
ν_a	Air kinematic viscosity
ν	Kinematic viscosity of the fluid
ρ	Density of the fluid
σ	Dimensionless surface charge density of the jet
$\bar{\sigma}$	Steady state profile of surface charge density
$\tilde{\sigma}$	Disturbance profile of surface charge density
τ	Stress tensor
τ_{zz}	Dimensionless axial component of stress tensor
τ_{rr}	Dimensionless radial component of stress tensor
τ^p	Polymer stress tensor
τ_{zz}^p	Dimensionless axial component of polymer stress tensor
τ_{rr}^p	Dimensionless radial component of polymer stress tensor
$\bar{\tau}_{zz}^p$	Steady state axial polymer stress tensor
$\bar{\tau}_{rr}^p$	Steady state radial polymer stress tensor
$\tilde{\tau}_{zz}^p$	Disturbance axial polymer stress tensor
$\tilde{\tau}_{rr}^p$	Disturbance radial polymer stress tensor
ϕ	Generic jet variable
$\bar{\phi}$	Steady state value of the generic jet variable

$\tilde{\phi}$	Disturbance profile for the generic jet variable
χ	Aspect ratio of the straight jet
ω	Temporal growth/decay rate of the imposed disturbances
ω_r	Real part of the disturbance growth rate
ω_i	Imaginary part of the disturbance growth rate
Λ	Extended/equilibrium backbone stretch ratio of XPP molecule